INDIAN JOURNAL OF SCIENCE AND TECHNOLOGY

RESEARCH ARTICLE

12 DOF Bipedal Robot Design: Kinematic Analysis and Dynamic Simulation

Ruchir J Desai[1,2], **Y D Patel**[3]*

1 Ph.D. Research scholar, The Charutar Vidya Mandal (CVM) University, Vallabh Vidyanagar, Gujarat, India
2 Assistant Professor, Mechanical Engineering Department, ADIT, The Charutar Vidya Mandal (CVM) University, New Vallabh Vidyanagar, Gujarat, India
3 Associate Professor and Head, Mechanical Engineering Department, ADIT, The Charutar Vidya Mandal (CVM) University, New Vallabh Vidyanagar, Gujarat, India

OPEN ACCESS

Received: 17-09-2024
Accepted: 27-12-2024
Published: 19-02-2025

Citation: Desai RJ, Patel YD (2025) 12 DOF Bipedal Robot Design: Kinematic Analysis and Dynamic Simulation. Indian Journal of Science and Technology 18(6): 390-402. https://doi.org/10.17485/IJST/v18i6.2938

* **Corresponding author**.

yashavantkumar.patel@cvmu.edu.in

Funding: None

Competing Interests: None

Published By Indian Society for Education and Environment (iSee)

ISSN
Print: 0974-6846
Electronic: 0974-5645

Abstract

Objectives: Bipedal robots are robotic systems designed to mimic the walking and balancing abilities on different terrain of humans. This paper represents detailed kinematic analysis and reference model-based control design for 12 Degrees of Freedom (DOF) bipedal manipulator. This study also evaluates the robot's stability and gait generation capabilities through dynamic simulations. **Methods:** A CAD model is developed and simulated in MATLAB/ Simulink/ Simscape multibody by considering the inverse kinematics, cubic polynomial trajectory, foot contact forces, step size and Center of Mass (COM). The Zero Moment Point (ZMP) is utilized to guarantee the static stability of the envisioned bipedal robot. **Findings:** The result of this analysis provides valuable insights into the design and control of bipedal robots with a high degree of freedom, paving the way for more advanced applications in the field of robotics. The robot replicates the walking pattern of the human on flat terrain by keeping COM at constant height of 0.904 m. **Novelty:** The proposed lower limb model is developed using anthropomorphic data and a comprehensive investigation of the development phases of bipedal robot has been evaluated. Moreover, descriptive analysis has been carried out for the movement of each joint angle which is derived from dynamic simulation.

Keywords: Bipedal Robot; Lower Limb; Kinematic Analysis; Gait Pattern; Simulation

1 Introduction

Forging the future of autonomy: Mobilizing robots to lead the charge in transformative advancements across manufacturing, agriculture, defense and space exploration. Mobile robots employ diverse locomotion mechanisms including wheeled, legged, tracked or articulated systems tailored to specific applications. Each type of locomotion system has its own set of advantages and disadvantages, making them suitable for different applications depending on specific requirements of task and environment. The Table 1 depicts comparison of different locomotion used in robotics.

Hence, the planning and management of mobile robots need a lot of attention. These robots grouped as legged robots, wheeled robots and tracks. The wheeled robots and tracks have disadvantages when compared to legged robots, which are workable on regular or irregular complex terrains, less energy consumption due to small contact area and the adaptability[1,2]. The legged robots are further sub divided into bipedal and multi-legged robots.

Table 1. Comparison of different locomotion used in robotics

	Wheeled	Legged	Tracked	Articulated
Type of surfaces	Smooth and flat	Highly adaptable to various terrains	Soft or uneven surface	Smooth, rough, and uneven terrains
Complexity of design	Simpler designs	Most complex	Complex	varying levels of complexity depending on the number of joints and DOF
Traction	Low	Average	Good	Excellent
Manoeuvrability	Good in structured terrains	Highest across various terrains and obstacles	Highest across various terrains and obstacles	Limited
Ability of orient	Limited	Highest	Good in tight spaces	Optimized
Speed	Fastest	Average	Good	Lowest
Stability	Low	Good	Superior	Moderate
Balancing	Straightforward balancing mechanisms	Advanced balancing mechanisms	Good at maintaining balance	Vary
Types of Obstacles can be traced	Small debris like pebbles or litter. Low curbs or small steps. Gaps or transitions between different floor surfaces (e.g., tile to carpet).	Stairs or steps. Uneven terrain with irregular surfaces. Gaps or narrow passages.	Large rocks or boulders. Steep inclines or declines. Mud, snow, or sand.	Adjusting their articulation to navigate through confined spaces. Tracing complex paths for assembly or inspection tasks.
Power requirement	Lower	Moderate to higher due to the number of legs, the weight of the robot, terrain roughness	Moderate to higher due to Continuous track motion and need for increased torque	Increases with the complexity of movements
Application examples	• Autonomous vehicles like cars and wheelchairs. • Domestic tasks, such as the Roomba vacuum cleaning robot. • Exploration, Transportation and production workshop. • Agriculture and environmental monitoring. • Defense and military operation.	• Reconnaissance and detection • Disaster prevention and rescue • Industrial patrol and inspection • Entertainment and sports	• Military • Search and Rescue • Agriculture • Space Exploration • Construction	• Manufacturing • Agriculture • Military and Defense • Education

The bipedal robot is meant to imitate human-like locomotion and perform bound tasks cherish activities in peril environments, assistances to the old, aged people and entertainment. The biped mechanism contains a trunk and legs with/without feet or perhaps entire human-like mechanism betting on specific applications. The biped robots have some advantages over multi-legged robots. It has significantly higher adaptability sanctionative them to simply surpass obstacles like narrow ways or stairs[3]. This adaptability is especially necessary once the robot is has to perform human-centred tasks. Thanks to the smaller ground contact space and fewer actuators used, their energy consumption may be less than multi-legged robots. This is often observed that two-legged animals have higher potency and flexibility than multi-legged animals.

A terrestrial locomotion system having two limbs is known as bipedal system[4]. The bipedal movement includes walking, running and hopping. The study of artificial arms and hands began in 1967 with the first aimed only to develop machines to perform manual labour in lieu of persons and emphasized development of artificial hand mechanisms. Recently the aim has been to develop robots which can perform intelligent work as well as manual labour.

There are several key challenges and limitations that still exist in the development of bipedal robots like energy efficiency, dynamic and adaptive gait planning, balance and stability control in dynamic environments, reducing production costs through simpler mechanical designs and standardized components. The present study addresses the overall development phases of the bipedal robots along with modelling and simulation of the full-scale robot to simplify the mechanical design and use of standardized components. The proposed design excels in dynamic, unstructured environments, enabling applications like search and rescue in disaster zones, hazardous industrial maintenance, complex manufacturing tasks, telerobotics for industries, defense and space exploration. Advancements in energy efficiency, AI, and durability will unlock their full potential across the above applications. This paper mainly focuses on the comprehensive study of the movement of each joint under the dynamic environment to achieve dynamic balance and stability. The next section presents the proposed bipedal robot model. This is followed by the kinematic modeling obtained using the Denavit - Hartenberg (DH) notations and inverse kinematics. Then, the biped leg position for different angles is verified using Peter-Corke robotics toolbox in Matlab® to see the possible movement and determine that it can be used for further analysis in the next phases i.e. dynamics and control each joint to get the desired motion.

2 Methodology

Development phases of Bipedal Robots

The development phases of bipedal robots include modelling of various manipulators and their configurations. It also includes various stability criteria, different control strategies, walking pattern generation. The analysis of these manipulators can be done by simulation as well as experiments. The first step in the development process is modelling and design.

2.1 Modelling and Design

It includes no. of degrees of freedom, no. of links, gait patterns, types of foot, type and location of joints and assembly of bipedal robot. An average human utilizes only about 20 DOF during motion, although there are more than 300 DOF available in the human musculoskeletal system. This fact enables humans to utilize various DOF that can be either locked or released, to adjust their motion patterns according to the environment and tasks at hand. Most researchers have sought to understand the principles of human walking by using various simplified models. The potential options available in literature for the lower limb robots: **2 – Links:** 1 leg consisting flexible links for thigh, knee and shin without foot having 2 DOF[5]. **4 – Link:** passive walking model having 3 DOF with shank and thigh in each leg with knee joint and without feet[6]. **5 – Links**: Sagittal plane model have 4 DOF consists of a trunk and two legs with knees, but without feet[7]. **7 – Links :** The robot consists of trunk, thigh, shin and metatarsal. The links are attached together by 6 revolute joints: two hip joints, two knee joints and two ankle joints[8]. **9 – Links**: Manipulator with a trunk consists of thigh, shin, and foot for each leg and has 3 DOF in the hip joint, one in the knee joint, and two in the ankle joint[9].

Modelling of the lower limb critically affects the robot's ability to move efficiently and maintain balance. The lower limb typically consists of foot, ankle joint, lower leg (calf), knee joint, upper leg (thigh), hip joint and torso which work together to enable the robot to walk and perform other movements. All these links are connected through revolute joint between them. The mechanical structure of the bipedal robot is developed using CAD software as shown in Figure 1 consists of 7 links and 12 DOF. The model consists of 3 revolute joints between torso and thigh for rolling, pitching and yawing motion. The joint between calf and thigh has 1 DOF to replicate the knee joint. The ankle joint between the calf and foot allows 2 DOF for rolling and pitching motion. One of the objectives here is to replicate the human walking pattern through the bipedal robot. Thus, the parameters in terms of ratios, range of motion, and physical length of the lower limb segments have been selected based on anthroponomics data available from Muscolo, 2017[10] as shown in Table 2.

Table 2. D-H parameters for the Right Leg

Joint	Link Name	a (Link Length)	α (Twist Angle)	d (Link Offset)	θ (Joint Angle)
1	Waist	0	90^0	0	θ_1
2	Waist-lateral	0	-90^0	0	-90^0
3	Waist-thigh	L3	0	0	θ_3
4	Knee	L4	0	0	θ_4
5	Ankle-lateral	0	90^0	0	θ_5
6	Ankle	L5	0	0	θ_6

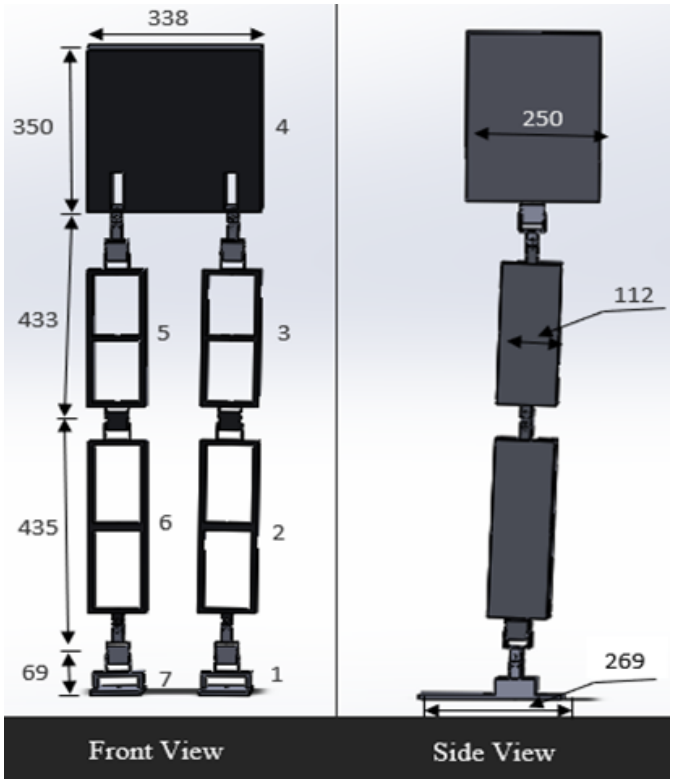

Fig 1. CAD model of the lower limb of the bipedal robot

The design of the lower limb is a complex process that requires careful consideration of factors such as range of motion, materials, and balance. As technology continues to evolve, one can expect to see increasingly sophisticated lower limb designs that enable bipedal robots to move with greater efficiency and agility.

2.1.1 Forward Kinematic Analysis

It is an important tool used in the design and control of bipedal robots. It involves analyzing the motion and movement of joints and limbs under the application of forces and torques acting on the robot's body. It can provide valuable insights into the robot's ability to maintain balance, walk efficiently, and perform other tasks. To perform this, the robot's joint angles and positions are measured and tracked over time. This data can be used to calculate the robot's velocity, acceleration, and other kinematic parameters. It can also be used to optimize the robot's gait and posture.

Table 3. Length and masses of various segments

The standard Indian Man (Age: 30; Height: 1720mm)			
Link No.	**Segment**	**Segment length (mm)**	**Segment mass (kg)**
1,7	Ankle to bottom of foot	69	
1,7	Foot breadth	97	0.49
1,7	Foot length	269	
2,6	Lower leg (calf)	435	0.87
3,5	Upper leg (thigh)	433	0.87
4	Hip width / leg separation (Trunk/ Torso)	338	1.9

Table 3 shows D-H parameters to perform direct kinematic analysis. x_0, y_0, z_0 at the center of the waist as the global reference frame and l_3, l_4 and l_5 denotes the length of different segments. The local frames as x_i, y_i, z_i have been attached to each links according to the D-H convention as described below.

1. *Rotate the frame x_{i-1}, y_{i-1}, z_{i-1} about the z_{i-1} axis through an angle θ_i .*
2. *Translate the current frame x_{i-1}, y_{i-1}, z_{i-1}along the current z_{i-1} axis by d_i units.*
3. *Translate the current frame x_{i-1}, y_{i-1}, z_{i-1} along the current x_i axis by a_i units.*
4. *Rotate the current frame x_{i-1}, y_{i-1}, z_{i-1} about the x_i axis through an angle α_i .*

Where a_i and d_i are the displacement along x and z axis respectively, α_i and θ_i are the angle of rotation about x and z axis respectively. As convention, the positions of each joint, shown in Figure 1 mean 0° angle. The angles are assumed positive, counterclockwise about the rotation axis. Note that the only parameters that vary are θ_i (joint angles of each leg). Since the kinematic structure of both the legs are same, for the convenience, right leg D-H parameters and matrix have been evaluated. When the robot is standing, the angle of each joint is the same for both the legs but as the robot starts walking, the angles may not remain same. To represent the coordinate system x_i in x_{i-1}, the previously obtained values can be used to compute the transformation. This involves applying two translations and two rotations.

The transforms matrix from x_{i-1} to x_i is given below. The link-to-link transformations are equal for both legs because two legs are identical:

$$A = Rot(z,\theta_{i+1}) * Trans\,(0,\,0,d_{i+1}) * Trans\,(a_{i+1},\,0,\,0) * Rot\,(x,\,\alpha_{i+1})$$

$$A = \begin{bmatrix} cos\theta & -sin\theta cos\alpha & sin\theta sin\alpha & acos\theta \\ sin\theta & cos\alpha cos\theta & -sin\alpha cos\theta & dsin\theta \\ 0 & sin\alpha & cos\alpha & d \\ 0 & 0 & 0 & 1 \end{bmatrix}$$

The transformation matrix of one leg and six degrees of freedom is given by,

$$[{}^0_6A] = [{}^0_1A] * [{}^1_2A] * [{}^2_3A] * [{}^3_4A] * [{}^4_5A] * [{}^5_6A] \; = \begin{bmatrix} n_x & s_x & a_x & P_x \\ n_y & s_y & a_y & P_y \\ n_z & s_z & a_z & P_z \\ 0 & 0 & 0 & 1 \end{bmatrix} \tag{1}$$

$$[{}^0_1A] = \begin{bmatrix} C_1 & 0 & -S_1 & 0 \\ S_1 & 0 & C_1 & 0 \\ 0 & -1 & 0 & 0 \\ 0 & 0 & 0 & 1 \end{bmatrix};\; [{}^1_2A] = \begin{bmatrix} C_2 & 0 & -S_2 & 0 \\ S_2 & 0 & C_2 & 0 \\ 0 & -1 & 0 & 0 \\ 0 & 0 & 0 & 1 \end{bmatrix};\; [{}^2_3A] = \begin{bmatrix} C_3 & -S_3 & 0 & L_3C_3 \\ S_3 & C_3 & 0 & L_3S_3 \\ 0 & 0 & 1 & p_z \\ 0 & 0 & 0 & 1 \end{bmatrix};$$

$$[{}^3_4A] = \begin{bmatrix} C_4 & -S_4 & 0 & L_4C_4 \\ S_4 & C_4 & 0 & L_4S_4 \\ 0 & 0 & 1 & 0 \\ 0 & 0 & 0 & 1 \end{bmatrix};\; [{}^4_5A] = \begin{bmatrix} C_5 & 0 & S_5 & 0 \\ S_5 & 0 & -C_5 & 0 \\ 0 & 1 & 0 & 0 \\ 0 & 0 & 0 & 1 \end{bmatrix};\; [{}^5_6A] = \begin{bmatrix} C_6 & -S_6 & 0 & L_5C_6 \\ S_6 & C_6 & 0 & L_5S_6 \\ 0 & 0 & 1 & 0 \\ 0 & 0 & 0 & 1 \end{bmatrix}$$

Where, $n_x = C_6 * (S_1 * (C_5 * C_4 * S_3 + C_5 * S_4 * C_3 + S_5 * C_4 * C_3)$
$+C_1 * C_2 * (C_5 * C_4 * C_3 - C_5 * S_4 * S_3 - S_5 * C_4 * S_3 * -S_5 * S_4 * C_3)) - C_1 * S_2 * S_6$

$s_x = -S_6 * (S_1 * (C_5 * C_4 * S_3 + C_5 * S_4 * C_3 + S_5 * C_4 * C_3)$
$+C_1 * C_2 * (C_5 * C_4 * C_3 - C_5 * S_4 * S_3 - S_5 * C_4 * S_3 - S_5 * S_4 * C_3)) - C_1 * C_6 * S_2$

$a_x = S_1 * (S_5 * (C_4 * S_3 + S_4 * C_3) - C_5 * (C_4 * C_3 - S_4 * S_3)) + C_1 * C_2 * (S_5 * (C_4 * C_3 - S_4 * S_3) - C_5 * (C_4 * S_3 + S_4 * C_3))$

$P_x = L_4 * S_4 * C_3 * S_1 - L_4 * S_4 * C_1 * C_2 * S_3 + L_3 * S_1 * S_3 + L_5 * C_6 * (S_1 * S_3 * C_4 * C_5 + C_1 * C_2 * C_3 * C_4 * C_5$
$+C_3 * S_1 * S_4 * C_5 - C_1 * C_2 * S_3 * S_4 * C_5 - S_1 * S_3 * S_4 * S_5 - C_1 * C_2 * C_3 * S_4 * S_5 + C_3 * S_1 * C_4 * S_5$
$-C_1 * C_2 * S_3 * C_4 * S_5) + L_4 * C_4 * S_1 * S_3 + L_4 * C_4 * C_1 * C_2 * C_3 + L_3 * C_1 * C_2 * C_3 - L_5 * C_1 * S_2 * S_6 P_x$
$= L_4 * S_4 * C_3 * S_1 - L_4 * S_4 * C_1 * C_2 * S_3 + L_3 * S_1 * S_3 + L_5 * C_6 * (S_1 * S_3 * C_4 * C_5 + C_1 * C_2 * C_3 * C_4 * C_5$
$+C_3 * S_1 * S_4 * C_5 - C_1 * C_2 * S_3 * S_4 * C_5 - S_1 * S_3 * S_4 * S_5 - C_1 * C_2 * C_3 * S_4 * S_5 + C_3 * S_1 * C_4 * S_5$
$-C_1 * C_2 * S_3 * C_4 * S_5) + L_4 * C_4 * S_1 * S_3 + L_4 * C_4 * C_1 * C_2 * C_3 + L_3 * C_1 * C_2 * C_3 - L_5 * C_1 * S_2 * S_6$

$$n_y = -C_6*(C_4*C_5*C_2*S_3 - S_4*S_5*C_1*S_3 + S_4*C_5*C_1*C_3 + C_4*S_5*C_1*C_3 - C_4*C_5*C_2*C_3*S_1 + S_4*S_5*C_2*C_3*S_1 + S_4*C_5*C_2*S_1*S_3 + C_4*S_5*C_2*S_1*S_3) - S_1*S_2*S_6$$

$$s_y = S_6*(C_4*C_5*C_1*S_3 - S_4*S_5*C_1*S_3 + S_4*C_5*C_1*C_3 + C_4*S_5*C_1*C_3 - C_4*C_5*C_2*C_3*S_1 + S_4*S_5*C_2*C_3*S_1 + S_4*C_5*C_2*S_1*S_3 + C_4*S_5*C_2*S_1*S_3) - C_6*S_1*S_2$$

$$a_y = C_1*C_3*C_4*C_5 - C_1*C_3*S_4*S_5 + C_2*S_1*S_3*C_4*C_5 - C_2*S_1*S_3*S_4*S_5 + C_2*C_3*S_1*S_4*C_5 + C_2*C_3*S_1*C_4*S_5 - C_1*S_3*S_4*C_5 - C_1*S_3*C_4*S_5$$

$$P_y = L_3*C_2*C_3*S_1 - L_3*C_1*S_3 - L_5*C_6*(C_4*C_5*C_1*S_3 - C_4*C_5*C_2*C_3*S_1 - S_4*S_5*C_1*S_3 + S_4*S_5*C_2*C_3*S_1) - L_5*C_6*(S_4*C_5*C_1*C_3 + S_4*C_5*C_2*S_1*S_3 + C_4*S_5*C_1*C_3 + C_4*S_5*C_2*S_1*S_3) - L_4*C_4*C_1*S_3 + L_4*C_4*C_2*C_3*S_1 - L_4*S_4*C_1*C_3 - L_4*S_4*C_2*S_1*S_3 - L_5*S_1*S_2*S_6$$

$$n_z = C_6*S_2*(S_3*S_4*C_5 + C_3*S_4*S_5 + S_3*C_4*S_5 - C_3*C_4*C_5) - C_2*S_6$$

$$s_z = -C_2*C_6 - S_6*S_2*(S_3*S_4*C_5 + C_3*S_4*S_5 + S_3*C_4*S_5 - C_3*C_4*C_5)$$

$$a_z = S_2*((S_3 - C_3)*S_5*C_4 - (S_3 + C_3)*C_5*S_4)$$

$$P_z = S_2*L_5*C_6*(S_4*(S_3 + C_3)*S_5 + C_4*(S_3 - C_3)*C_5) - S_2*L_3*C_3 - S_2*L_4*C_3*C_4 + S_2*L_4*S_3*S_4 - L_5*C_2*S_6$$

2.1.2 Inverse Kinematics

The inverse kinematic analysis has been done in reverse order calculation of the transformation matrix. In this paper, the closed-form solutions of the kinematic equations are used which was proposed by Pieper. The proposed method suggests that the manipulator's joint solution exists only if the three adjacent joint axes are intersecting at a single point, or they are parallel to one another. The transformation matrix for inverse kinematics for 12 DOF robot is developed in the reverse order such that foot as base and the hip as end effector. It is decoupled into two subsystems i.e. positioning (first three joint angles: θ_4, θ_5 and θ_6) and orientation (last three joint angles: θ_1, θ_2 and θ_3).

The inverse transformation matrix of Equation (1) can be given by,

$$[{}^0_6A] = [{}^5_6A]*[{}^4_5A]*[{}^3_4A]*[{}^2_3A]*[{}^1_2A]*[{}^0_1A] \tag{2}$$

$$p_x = L_5 - L_3*(C_6*S_4*S_5 - C_4*C_5*C_6) + L_4*C_5*C_6 \tag{3}$$

$$p_y = L_4*C_5*S_6 - L_3*(S_4*S_5*S_6 - C_4*C_5*S_6) \tag{4}$$

$$p_z = L_3*(C_4*S_5 + C_5*S_4) + L_4*S_5 \tag{5}$$

The Equations (3), (4) and (5) can be obtained by Equation (2) and represent inverse transformation matrix. These equations are used to get the joint angles for each leg i.e. θ_4, θ_5 and θ_6 as given below.

$$C_4 = \frac{(p(1)+L_5)^2 + p(2)^2 + p(3)^2 - {L_3}^2 - {L_4}^2}{2*L_3*L_4}$$

$$temp = (p(1)+L_5)^2 + p(2)^2$$

$$\theta_4 = atan2(\sqrt{temp}, C_4) \tag{6}$$

$$\theta_5 = atan2(-p(3), \sqrt{temp}) - atan2(S_4*L_3, C_4*L_3 + L_4) \tag{7}$$

$$\theta_6 = atan2(p(2), -p(1) - L_5) \tag{8}$$

$$temp = 1 - (S_6 * a(1) + C_6 * a(2))^2$$

The Equations (6), (7) and (8) give the values of the knee, ankle roll and pitch joint angles respectively, obtained from closed form kinematic solution. The other three joint angles θ_1, θ_2 and θ_3, can be obtained by following method. The inverse transform matrix $[{}^6_5A]$ is to be moved to the left-hand side of Equation (2).

$$T' = \begin{bmatrix} n & s & a & p \\ 0 & 0 & 0 & 1 \end{bmatrix}^{-1} = \begin{bmatrix} n' & s' & a' & p' \\ 0 & 0 & 0 & 1 \end{bmatrix}$$

$$= [{}^6_5A] * [{}^5_4A] * [{}^4_3A] * [{}^3_2A] * [{}^2_1A] * [{}^1_0A] = [{}^6_0A] \tag{9}$$

$$LHS = [{}^5_6A] * \begin{bmatrix} n' & s' & a' & p' \\ 0 & 0 & 0 & 1 \end{bmatrix} \tag{10}$$

$$RHS = [{}^5_4A] * [{}^4_3A] * [{}^3_2A] * [{}^2_1A] * [{}^1_0A] \tag{11}$$

The Equations (10) and (11) represent Left-Hand Side and Right-Hand Side of the Equation (9). Thus, by solving these two sides of the equation, the unknown joint angles can be obtained as below.

$$\theta_2 = atan2(-\sqrt{temp}, S_6 * a(1) + C_6 * a(2)) \tag{12}$$

$$\theta_1 = atan2(-S_6 * s(1) - C_6 * s(2), -S_6 * n(1) - C_6 * n(2)) \tag{13}$$

$$\theta_{345} = atan2(a(3), C_6 * a(1) - S_6 * a(2))$$

$$\theta_3 = \theta_{345} - \theta_4 - \theta_5 \tag{14}$$

The Equations (12), (13) and (14) represent the joint angles of hip roll, yaw and pitch respectively. These equations are further used to evaluate the trajectory of a biped mechanism.

2.2 Stability criterion

The stability criteria are of two types, i.e. static and dynamic, which influence the trajectory of a biped mechanism. Static stability requires the vertical projection of the biped's COM stays within the boundaries of the support polygon [11]. The support polygon is the area defined by the points of contact the biped has with the ground. For example, if a biped is standing on one foot, the support polygon is just the area under that single foot. If it's standing on two feet, the support polygon is the area between the two feet [11]. Thus, static stability provides slow gait with large feet of bipedal manipulator. Dynamic stability offers greater flexibility compared to static, as it allows the projected COM to move outside the support polygon. This enables faster and more dynamic gaits [12].

In this work, the ZMP approach is used to generate a stable walking pattern and control a robot. Moreover, it is desired for bipedal to walk without tipping over against single and double support phases, the manipulator needs to generate a reaction

moment to counteract the overturning moment created by COM[13]. This reaction arises from the contact force between the foot and the ground. The point on the foot where this reaction force acts is known as the ZMP[14]. It is important to find the position of ZMP during the walk because the position of the point keeps changing according to the SSP and DSP. The following equations are used to obtain the position of ZMP in X and Y axis, Z axis is in the upward direction.

$$x_{zmp} = x_{com} - \frac{z_{com}}{g} * \ddot{x}_{com} \tag{15}$$

$$y_{zmp} = y_{com} - \frac{z_{com}}{g} * \ddot{y}_{com} \tag{16}$$

Figure 2 illustrates the oscillation of COM, reference trajectory of ZMP, and steps taken by the robot during walking. The location of ZMP is constrained by the distance between the robot's two legs. If this constraint is exceeded due to the position of COM, robot may become unstable and potentially topple over[15]. To avoid exceeding this limit, it is essential to control the joint movements of a bipedal, as these movements affect the position of COM.

To ensure stability according to ZMP, the walking pattern design should maintain continuous contact between stance foot and the ground throughout the walking motion. In addition, the design of manipulators includes six revolute joints per leg which are all actuated by individual electric motors and controlled to track predetermined trajectories. The trajectory of the bipedal is developed by considering the walking pattern based on the linear inverted pendulum model (LIPM) that can simplify the control task during the SSP.

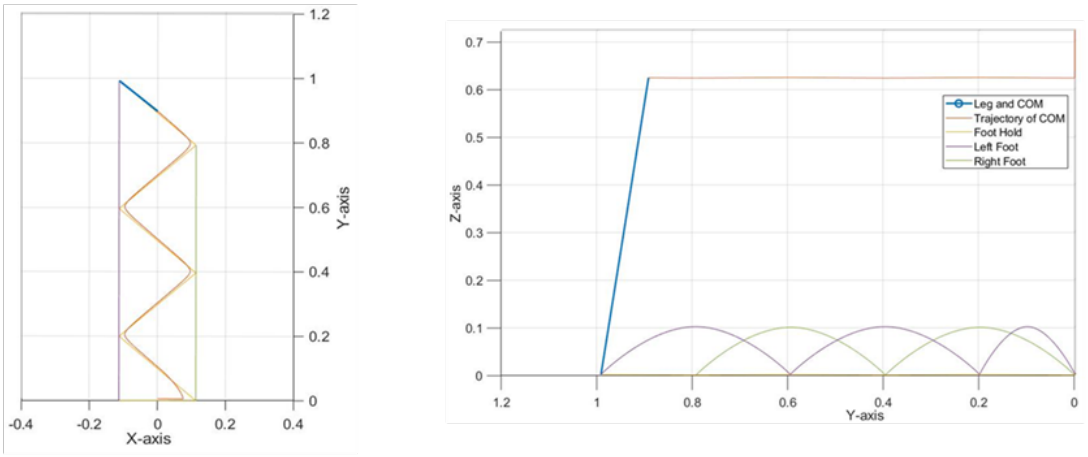

(a) Top View (b) Front View

Fig 2. COM and ZMP reference trajectories of bipedal robot walking in top view and front view

2.2.1 Controlling strategies

One of the key challenges in bipedal locomotion is generating desired paths that maintain stability while also avoiding collisions with obstacles[16]. Because biped robots and human locomotion share similarities, certain important aspects must be considered to achieve natural and effective bipedal movement. The real-time deep learning-based model predictive control (MPC) approach have been initially developed and tested for a 3-DOF biped leg by some researchers[17]. In this work, the model-based gait method is used to generate reference trajectories of joints for bipedal. This method adopts ZMP and periodicity as stability criteria and provides information about the behavior of human walking. Moreover, the model-based gait system guarantees dynamic stability. Then a robust control system is performed to track the desired trajectories[18].

2.3 Walking pattern generators

2.3.1 Human Locomotion

In human walking, the gait cycle is divided into two primary phases: stance and swing. During the stance phase, the foot is in contact with the ground, supporting body progression and maintaining an upright posture. In contrast, the swing phase occurs when the foot is airborne, allowing the leg to advance and preparing for the next step. Typically, stance phase constitutes about 60% of the gait cycle, while the swing phase makes up approximately 40% [19].

2.3.2 Gait Pattern

The stance phase can be further divided into two sub-phases: SSP and DSP. DSP occurs when both feet are in contact with the ground, creating a closed-chain mechanism. SSP begins when the rear foot lifts off the ground and the front foot remains in contact. Typically, DSP constitutes about 20% of the time during one stride of gait, while SSP accounts for approximately 80% [20].

Thus, the complete gait cycle in human walking comprises two main successive phases. During SSP, the bipedal experiences instability due to under-actuation caused by the passive nature of the foot-ground contact. Essentially, controlling the feet relies on managing the mechanism above them. The researchers have identified various patterns used for generating periodic bipedal walking. The complex gait pattern consists of four phases of one complete cycle which includes two sub-phases of SSP and DSP each [21]. This pattern arises the need for additional DOF at the foot. Some researchers have followed the three-stage pattern. It includes two sub-phases of DSP and one phase of SSP [22]. This paper uses two-step gait patterns, successive DSP and SSP without sub-phases to enhance stability and simplify walking pattern generation. The swing feet stay parallel to the ground during lift-off and landing, maximizing ground support and keeping the ZMP within the stance foot's contact area, ensuring static stability with the COM's vertical projection within the support polygon.

2.4 Simulation

Biped robots with human-like joint dynamics can be effectively simulated in MATLAB/Simulink, using Newtonian dynamics for force and torque. Simscape multibody library simplifies modeling these robots. To mimic human movement, it's essential to match human body proportions [23]. Figure 3 displays a simulation model of the biped robot, including the torso, upper leg, lower leg, and foot, with a swing height of 0.1 m. The robot walks with a constant step length of 0.2 m after an initial half step, completing seven steps in ten seconds. The model's total height is 1.004 m, with the center of mass at 0.904 m.

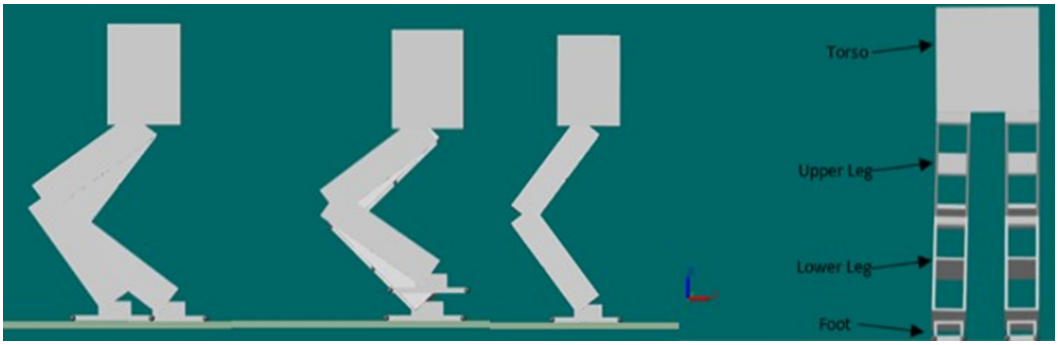

Fig 3. Simulation of the Biped mechanism including front view, side view, swing height of the leg and one step walking (from right to left)

Figure 4 shows a Simulink model for simulating walking dynamics. The "World Plane" block sets the reference frame for the robot's ground plane. This model captures interactions between the robot's legs and torso during locomotion. The torso is the upper body, while the left and right leg blocks receive control signals from inverse kinematics to dictate foot trajectories and leg movements. The control system block includes algorithms to manage the robot's gait for stable walking. Sensors and measurement blocks provide feedback for real-time adjustments. Overall, this model integrates physical and control elements to simulate bipedal walking effectively.

Figure 5 shows a Simulink model of a bipedal robot, focusing on the Hip, Knee, and Ankle Joints. The core is the contact system, representing foot-ground interaction and its effect on movement. The ankle connects the foot to the lower leg, which links to the upper leg via the knee joint, and to the torso through the hip joint. These joints are essential for simulating human-

like walking. Each joint block has sensors that measure key parameters for real-time feedback and control, enabling dynamic adjustments and precise simulation of the robot's gait. Overall, the model provides a detailed framework for simulating the walking behaviour of robot. It integrates trajectory planning, inverse kinematics, joint control, and real-time feedback to achieve stable and coordinated walking.

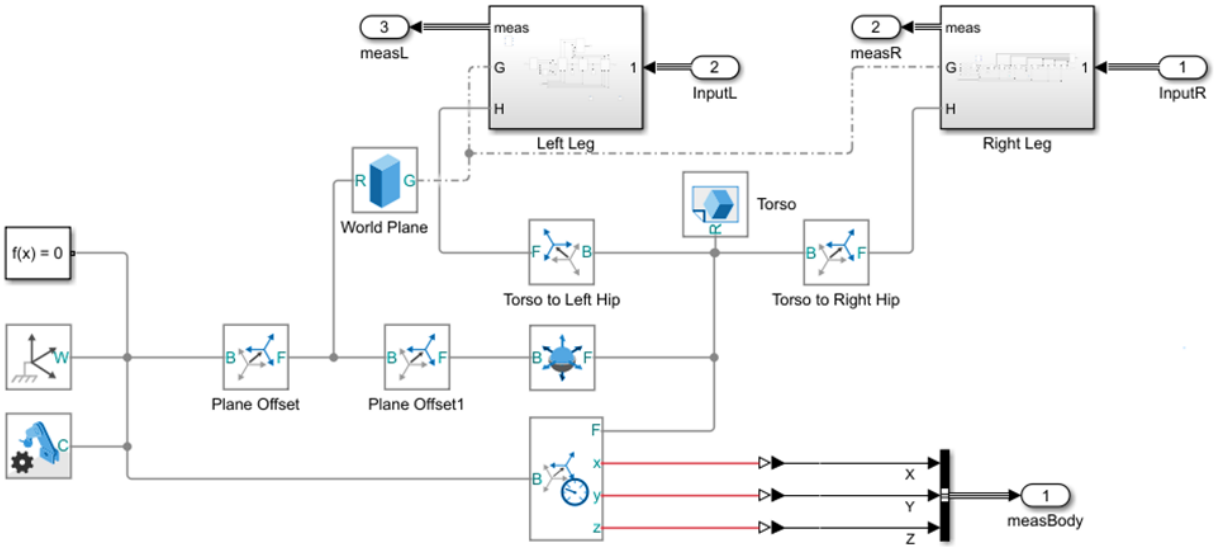

Fig 4. Development of a Robot structure using Simulink

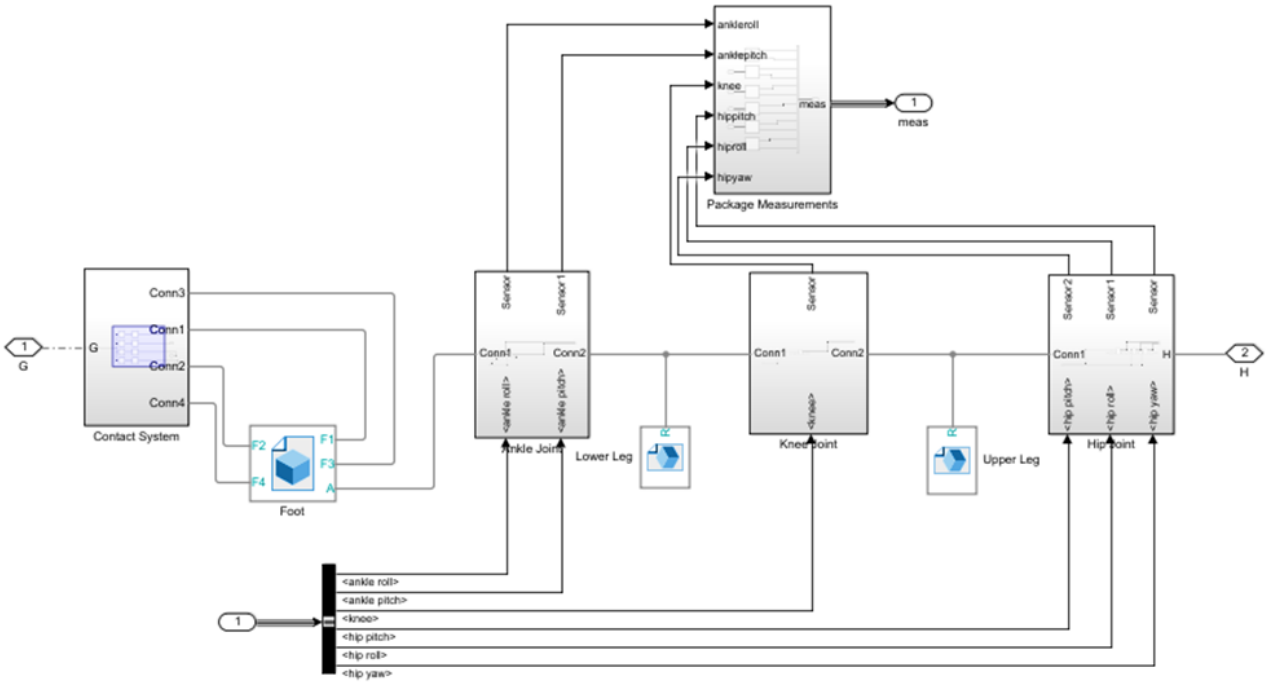

Fig 5. Joint created between the two links i.e. Hip Joint, Knee Joint and Ankle Joint of Bipedal robot

3 Result and Discussion

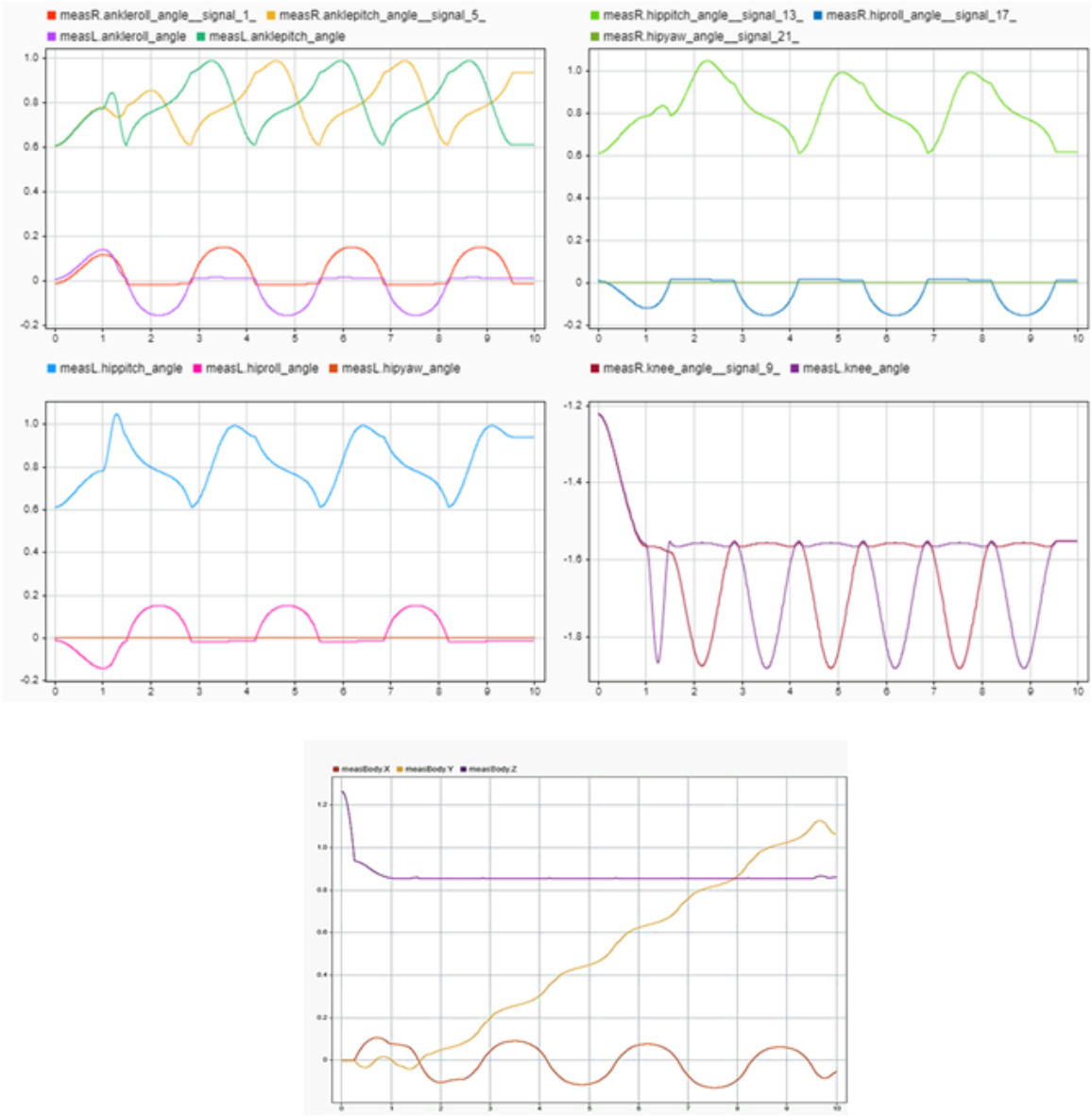

Fig 6. (a) Ankle angles, (b) Right Hip angles, (c) Left Hip angles, (d) Knee angles and (e) Robot body movement

Figure 6 **(a)** displays variations in left and right ankle roll and pitch angles over 10 seconds. The right ankle roll angle oscillates with a peak amplitude of 0.15 radians, while the left ankle roll angle oscillates with smaller peaks. Both ankle pitch angles oscillate with a peak amplitude of 1.0 radians and a minimum of 0.6 radians. The oscillation period for all angles is around 2.6 seconds. This plot shows synchronized ankle movements during walking or running, with symmetrical angles indicating natural gait patterns. Larger pitch angle oscillations compared to roll angles highlight the importance of forward-backward movement for stability.

Figure 6 **(b)** shows right leg hip angles for pitch, roll, and yaw. The hip pitch angle oscillates between 0.6 and 1.0 radians, the roll angle peaks at -0.15 radians, and the yaw angle remains near zero with minimal movement. Overall, the hip angle

exhibits periodic behavior with a 2.6-second period. The pitch angle has the largest oscillations, reflecting significant forward-backward movement, while the roll angle shows smaller amplitude, indicating less side-to-side movement. The stable yaw angle suggests minimal rotational movement, consistent with expected locomotion patterns. The analysis of hip and ankle pitch angles shows a coordinated, efficient gait with consistent motion and synchronization between joints, indicating effective balance and propulsion during walking. Figure 6 **(c)** illustrates the left hip angles-pitch, roll, and yaw-over 10 seconds. The pitch angle oscillates with a 1.0-radian amplitude, the roll angle peaks around 0.15 radians, and the yaw angle remains near zero with minimal fluctuations. These patterns suggest repetitive movements typical of walking or running. The pitch angle exhibits the most significant movement, reflecting forward propulsion, while the roll angle adjusts for side-to-side balance, and the stable yaw angle indicates minimal rotational movement.

Knee angles show initial transients before settling into regular oscillations represented in Figure 6**(d)**, with both knees exhibiting decreasing amplitude over time, suggesting improved stability and control. This behavior aligns with theoretical models of bipedal locomotion, emphasizing alternating leg movements. Differences in frequency and damping between knees may be due to design symmetries. Understanding the knee angles over time can enhance the robot's overall gait stability and performance. The displacement (Figure 6 **(e)**) of robot in X-axis shows increasing oscillations, Y-axis trends upwards steadily, and Z-axis stabilizes quickly around 0.83 meters. The X-axis wave-like pattern indicates lateral movements during the robot's walk, with increasing amplitude suggesting potential instability or periodic balance adjustments. Initial small oscillations followed by larger swings reflect stabilization efforts. The Y-axis displacement shows forward movement with minor fluctuations from stepping. Initial large Z-axis displacement stabilizes to nearly zero, indicating vertical adjustment and successful stabilization. Consistent small Z-axis oscillations suggest the robot maintains a steady height of 0.83 m with minor vertical adjustments. The observed trends match bipedal locomotion behaviors: X-axis lateral oscillations reflect shifting mass, Y-axis steady forward movement with minor stepping fluctuations, and Z-axis stabilization indicates effective height control. The results indicate good gait stability and control, with lateral oscillations suggesting a need for improved control algorithms, successful vertical stabilization, and consistent forward locomotion. Differences in leg performance or external disturbances might contribute to the observed patterns.

The results obtained are more realistic while compared to Singh et al [24] due to the anthropometric data is used in the simple design of the full scaled model. The dynamic stability and more efficient motion profile is simulated in the present work unlike the static design simulations in [24]. The motion dynamics of the present study indicates 0 to 10 sec period with an improved locomotion and force distribution compared to the same analyzed by Bravo et al with only 2 sec period. The simulation model developed by [25], is for only seven DOF robot as compared to 12 DOF in the present work.

4 Conclusion

Kinematic analysis of bipedal robot with 12 DOF has yielded valuable insights into its motion capabilities and trajectory planning. By examining the various joint angles and constraints that influence the robot's movement, one can optimize its performance and stability while walking or running.

The comprehensive study of the joint movement indicates that maximum fluctuation of 0.65 radians is observed at the knee joints and minimum fluctuation at hip yaw joint. The robot walks on a flat surface by keeping 0.904 m of constant height of the COM. This analysis is essential for designing advanced control algorithms and development of robust locomotion strategies, enabling bipedal robots to excel in diverse applications, such as search and rescue missions, exploration in hazardous environments, and assistance in healthcare or industrial settings. The key findings of this analysis, such as optimal joint configurations and the effects of specific constraints on mobility, pave the way for more efficient and agile robotic systems. Furthermore, this foundational work opens avenues for future research, including the integration of machine learning techniques for adaptive locomotion and the exploration of bio-inspired designs. Overall, kinematic analysis not only enhances our understanding of bipedal motion but also serves as a critical stepping stone toward the advancement of robotics in real-world scenarios.

References

1) Tang J, Zhu Y, Gan W, Mou H, Leng J, Li Q, et al. Design, control, and validation of a symmetrical hip and straight-legged vertically-compliant bipedal robot. *Biomimetics*. 2023;8(4):1–22. Available from: https://doi.org/10.3390/biomimetics8040340.
2) Rahman MH, Islam MM, Al-Monir MF, Alam SB, Ruzbelt. Kinematics analysis of a quadruped robot: simulation and evaluation. In: 2022 2nd International Conference on Image Processing and Robotics (ICIPRob). 2022;p. 1–6. Available from: https://doi.org/10.1109/ICIPRob54042.2022.9798744.
3) Al-Shuka H, Corves B, Zhu WH, Vanderborght B. Multi-level control of zero-moment point-based humanoid biped robots: a review. *Robotica*. 2015;1(11):1–27. Available from: http://dx.doi.org/10.1017/S0263574715000107.

4) Grizzle JW, Chevallereau C, Sinnet RW, Ames AD. Models, feedback control, and open problems of 3D bipedal robotic walking. *Automatica*. 2014;50(8):1955–1988. Available from: https://doi.org/10.1016/j.automatica.2014.04.021.
5) Fazel R, Shafei AM, Nekoo SR. Kinematic analysis of flexible bipedal robotic systems. *Applied Mathematics and Mechanics*. 2024;45:795–818. Available from: https://doi.org/10.1007/s10483-024-3081-8.
6) Wang H, Chen Y. Simulation analysis of a passive biped robot. *Frontiers in Science and Engineering*. 2024;4(9):96–102. Available from: https://doi.org/10.54691/y9gqez85.
7) Kakaei MM, Salarieh H. New robust control method applied to the locomotion of a 5-link biped robot. *Robotica*. 2020;38(11):2023–2038. Available from: https://doi.org/10.1017/S0263574719001796.
8) Huang Q, Yokoi K, Kajita S, Kaneko K, Arai H, Koyachi N. Planning walking patterns for a biped robot. *IEEE Trans Robot Autom*. 2001;17(3):280–289.
9) Fattah A, Fakhari A. Trajectory planning of walking with different step lengths of a seven-link biped robot. In: Proceedings of the ASME 2010 International Design Engineering Technical Conferences and Computers and Information in Engineering Conference;vol. 2 of 34th Annual Mechanisms and Robotics Conference, Parts A and B. 2010;p. 1361–1369. Available from: https://doi.org/10.1115/DETC2010-28626.
10) Muscolo GG, Caldwell D, Cannella F. Biomechanics of human locomotion with constraints to design flexible-wheeled biped robots. In: 2017 IEEE International Conference on Advanced Intelligent Mechatronics (AIM). 2017;p. 1273–1278. Available from: https://doi.org/10.1109/AIM.2017.8014193.
11) Goswami A. Postural stability of biped robots and the foot-rotation indicator (FRI) point. *International Journal of Robotics Research*. 1999;18(6):523–533. Available from: https://doi.org/10.1177/02783649922066376.
12) Nicholls E. Bipedal dynamic walking in robotics [Honors thesis]. 1998. Available from: http://robotics.ee.uwa.edu.au.
13) Grizzle JW, Chevallereau C, Sinnet RW, Ames AD. Models, feedback control, and open problems of 3D bipedal robotic walking. *Automatica*. 2014;50(8):1955–1988. Available from: https://doi.org/10.1016/j.automatica.2014.04.021.
14) Kar DC, Issac KK, Jayarajan K. Gaits and energetics in terrestrial legged locomotion. *Mech Mach Theory*. 2003;38(4):355–366. Available from: https://doi.org/10.1016/S0094-114X(02)00124-6.
15) Khusainov R, Shimchik I, Afanasyev I, Magid E. Toward a human-like locomotion: modelling dynamically stable locomotion of an anthropomorphic robot in Simulink environment. In: Proceedings of the 12th International Conference on Informatics in Control, Automation and Robotics. 2015;p. 141–148. Available from: https://doi.org/10.5220/0005576001410148.
16) Vundavilli PR, Pratihar DK. Gait planning of biped robots using soft computing: an attempt to incorporate intelligence. In: Studies in Computational Intelligence. Singapore. Springer. 2010;p. 57–85. Available from: https://doi.org/10.1007/978-3-642-11676-6_4.
17) El-Hussieny H. Real-time deep learning-based model predictive control of a 3-DOF biped robot leg. *Scientific Reports*. 2024;14:16243. Available from: https://doi.org/10.1038/s41598-024-66104-y.
18) Vanderborght B, Van Ham R, Verrelst B, Van Damme M, Lefeber D. Overview of the Lucy project: dynamic stabilization of a biped powered by pneumatic artificial muscles. *Advanced Robotics*. 2008;22(10):1027–1051. Available from: https://doi.org/10.1163/156855308X324749.
19) Torricelli D, Gonzalez J, Weckx M, Jiménez-Fabián R, Vanderborght B, Sartori M. Human-like compliant locomotion: state of the art of robotic implementations. *Bioinspiration & Biomimetics*. 2016;11(5):51002. Available from: https://doi.org/10.1088/1748-3190/11/5/051002.
20) Al-Shuka HFN, Allmendinger F, Corves B, Zhu WH. Modeling, stability and walking pattern generators of biped robots: a review. *Robotica*. 2014;32(6):907–934. Available from: https://dx.doi.org/10.1017/s0263574713001124.
21) Chevallereau C, Bessonnet G, Abba G, Aoustin Y. Bipedal Robots, modeling, design and building walking robots. Malden MA. John Wiley. 2009. Available from: https://www.researchandmarkets.com/.
22) Huang Q, Yokoi K, Kajita S, Kaneko K, Arai H, Koyachi N, et al. Planning walking patterns for a biped robot. *IEEE Transactions on Robotics and Automation*. 2001;17(3):280–289. Available from: https://dx.doi.org/10.1109/70.938385.
23) Thakkar AM, Patel VJ. Walking Simulation of Biped Robot: A MATLAB/Simulink Module Approach. *Indian Journal Of Science And Technology*. 2024;17(1):47–58. Available from: https://dx.doi.org/10.17485/ijst/v17i1.2500.
24) Singh R, Kukshal V, Yadav VS. Mathematical Modelling, Design and Simulation of a Bipedal Walker. In: Smart Innovation, Systems and Technologies. Singapore. Springer. 2021;p. 531–544. Available from: https://doi.org/10.1007/978-981-15-9829-6_42.
25) M DAB, Rodas CFR. Design of a Dynamic Simulator for a Biped Robot. *Modelling and Simulation in Engineering*. 2021;2021:1–12. Available from: https://dx.doi.org/10.1155/2021/5539123.